Electronic Immunoaffinity Assay for Differential Leukocyte Counts

Ruxiu Liu, A K M Arifuzzman, Ningquan Wang, Ozgun Civelekoglu, and A. Fatih Sarioglu, *Member, IEEE*

***Abstract*—Leukocytes are blood cells involved in the immune response. Leukocytes can be classified into three main groups (granulocytes, lymphocytes, and monocytes), and the measurement of the relative prevalence of each subgroup, termed differential leukocyte count, is an important clinical parameter in the diagnosis and prognosis of various health anomalies. Currently, differential leukocyte counts are obtained either manually through labor-intensive blood smears or by employing bulky hematology analyzers. Both of these measurements require a laboratory setup and hence are not amenable for decentralized and point-of-care settings. In this paper, we introduce a microfluidic assay with an electronic readout for differential leukocyte count assays. Our device classifies leukocyte subgroups based on the differential CD33 expression on cell membranes. In the device, each subgroup is differentially immunocaptured in different microfluidic chambers, while the cell capture rates are quantified by an integrated electronic sensor network. When benchmarked against a commercial hematology analyzer, our device could identify leukocyte subpopulations with differences of <6% for granulocytes and lymphocytes, and a <3% for monocytes. These results demonstrate the potential of our technique as an accurate method to perform the widely-employed hematology assay for point-of-care applications without the need for sample labeling.**

***Index Terms*—complete blood count, differential leukocyte count, lab-on-a-chip, microfluidic CODES, microfluidics, surface antigens.**

I. Introduction

LEUKOCYTES are blood cells centrally involved in immune response, and therefore, are commonly profiled for diagnosis or prognosis of health conditions. Leukocytes can be classified into three main groups, namely granulocytes, lymphocytes, and monocytes, based on their biophysical and biochemical characteristics. The relative prevalence of each subpopulation, called differential leukocyte count, is a widely employed blood test as part of a routine medical examination, and can be used to diagnose health disorders, e.g., monocytosis (an increase in monocyte population) indicates chronic inflammations caused by tuberculosis or malaria, or some systemic autoimmune diseases such as systemic lupus erythematosus [1,2]; lymphocytopenia (a decrease in lymphocyte population) may point to inherited immune deficiency, blood cell dysfunction, or infectious diseases caused by viruses, bacteria, or parasites [3].

Currently, the differential leukocyte count is conventionally analyzed through the complete blood count (CBC) test using bulky hematology analyzers, or through microscopic examination of blood smears by a technician. These two approaches both need to be performed in a centralized, staffed laboratory settings and therefore cannot address the testing needs in point-of-care and/or resource-limited mobile settings.

Microfluidic devices have been developed as blood-based assays offering the advantage of screening blood cells in a well-controlled microenvironment [4]. In a flow cytometer, microfluidic channels can be used to drive fluorescently labeled leukocytes through a focused laser beam as scattered light and fluorescence emission are measured with optical sensors for cell classification [5-8]. Employing microfluidic components

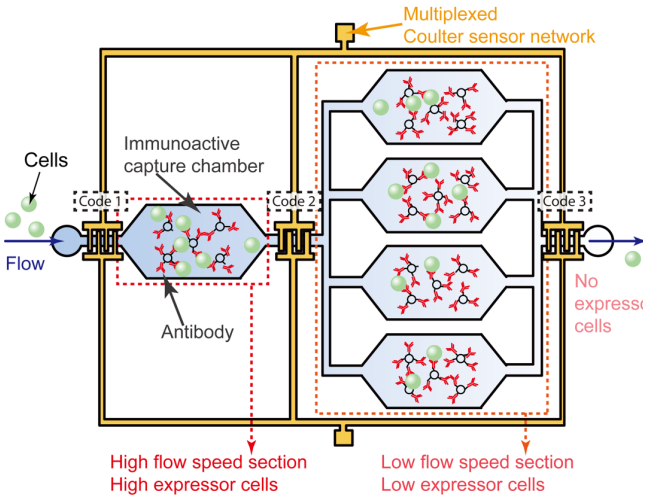

Fig. 1. A schematic showing the operation of the device. All the microfluidic cell capture chambers are functionalized with the same antibody (anti-CD33). Cells expressing different levels of the target antigen are immunocaptured in the chambers under different flow speeds, which are regulated by the total cross-sectional area in each section. The flow rate in the 1st chamber is 4× of the flow rate in the subsequent array of 4 chambers. The number of captured cells in each chamber is determined by an on-chip network of electrical sensors placed at strategic nodes across the device.

Manuscript received XXX.

This work was supported in part by the Arnold and Mabel Beckman Foundation (Beckman Young Investigator Award to A.F.S.) and the National Science Foundation under Grants ECCS 1752170.

The authors are with the School of Electrical and Computer Engineering, the Georgia Institute of Technology, Atlanta, GA 30332 USA (email: sarioglu@gatech.edu).

Color versions of one or more of the figures in this paper are available online at http://ieeexplore.ieee.org.

help miniaturization of flow cytometers; however, external optical components still complicate the system integration. Alternatively, electrical sensors can be used for cell identification through cell-induced changes in electrolyte impedance [9] or from impedance spectra within a frequency band [10-12]. Relying on electrical characterization allows label-free measurements and simplifies the instrument, but lacks the specificity of biochemical markers.

In this paper, we introduce a microfluidic device that can electrically provide differential leucocyte count by exploiting the differences in membrane antigen expression between leukocyte subpopulations. Specifically, we first spatially separate leukocytes on the microfluidic chip by immunocapturing cells with different antigen expression levels at different locations. Spatial distribution of cells on the device is then captured electrically by an integrated network of coded Coulter counters, and differential leukocyte count is obtained. Our technique does not require pre-labeling of leukocytes and provides an accurate, portable, and simple-to-use leukocyte test that can be performed at resource-limited and point-of-care settings.

II. Device Design, Operation, And Fabrication

Our device consisted of a microfluidic layer patterned to form an array of leukocyte capture chambers, and a glass substrate with micromachined gold electrodes that form the code-multiplexed Coulter sensor network (Fig. 1). The leukocyte capture chamber array can be considered as two sections: the first section includes a single chamber and is followed by the second section with four identical capture chambers. Each cell capture chamber measures 9 mm in length and 3 mm in width, and contains circular pillars that are arranged as a staggering array to increase the likelihood of the contact between cells and the device. Two sections are connected with a microfluidic channel that distributes the cells discharged from the single chamber in the first stage into the four parallel chambers in the second stage. This arrangement results in cells flowing at 4× reduced speed at the second stage compared to the first stage. The dimensions of the device and microfluidic capture chambers were designed based on the anticipated number of the cells to be immunocaptured. Specifically, a differential leukocyte count requires an analysis of ~10^3-10^4 cells for statistical power. Therefore, we designed our microfluidic chambers large enough to accommodate >10^4 cells with minimal steric hindrance in the immunocapture.

To differentially capture leukocytes at different locations in our device, microfluidic chambers are chemically functionalized with antibodies that target CD33. Among various antigens expressed by leukocytes, we chose CD33 as the target since CD33 is expressed by all leukocyte subpopulations at different levels [13]. Through flow cytometry, we measured the CD33 expression level among other antigens and determined that CD33 was a suitable surface marker for our application, because it is expressed at distinguishable levels between different leukocyte subpopulations (Fig. 2). Therefore, when a leukocyte suspension was driven through our anti-CD33-functionalized device, high CD33 expressors (i.e., monocytes) in the first section were captured where the flow was fast, while low expressors (i.e., granulocytes) were captured in the second section under the reduced flow rate. This is because, the immunocapture of cell is a probabilistic process with the possibility of a cell being captured is a function of the number of cell membrane antigens and the duration of the antibody-antigen interaction, which controlled by the sample flow speed [14,15]: a faster flow speed requires more antibody-antigen binding sites for a complete capture process, but provides shorter time for the reaction, so cells with higher antigen expression will be captured in the higher flow speed section. Finally, the cells that were not captured on the device were considered as lymphocytes with virtually absent CD33 expression.

To electrically count cells captured in each cell capture section, we used the Microfluidic CODES [16,17], a multiplexed biosensor technology for distributed Coulter detection on microfluidic chips. Microfluidic CODES uses micropatterned Coulter sensors to produce distinct waveforms at strategic nodes in a microfluidic device and allows electrical monitoring of cell capture dynamics from a single electrical waveform [18, 19]. Accordingly, we placed distinctly encoded Coulter sensors at specifically chosen locations across the device to quantify the cell capture rates in individual capture regions. Sensors were patterned to produce orthogonal Gold sequences [20-22], so that data from individual sensors can be

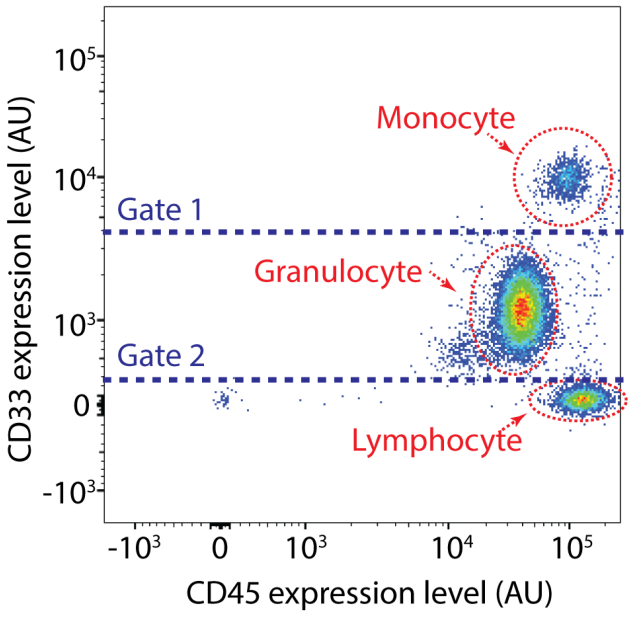

Fig. 2. Classification of leukocyte based on CD33 expression level with flow cytometry. The figure shows the heat map of the CD33 expression level on leukocytes. The x-axis represents the expression level of CD45 (leukocyte common antigen, which is expressed on all leukocytes), and the y-axis represents the expression level of CD33 on individual leukocytes analyzed. The expression level is measured from the intensity of fluorescence emission from leukocytes labeled with fluorophore conjugated anti-CD45 and anti-CD33 antibodies. The cells are then clustered into leukocyte subpopulations according to their expression levels. The result shows clear CD33 expression level boundaries (Gate 1 and Gate 2) between three leukocyte subpopulations.

TABLE I
THE GOLD CODES USED IN THE MULTIPLEXED SENSOR NETWORK FOR THE MICROFLUIDIC DIFFERENTIAL LEUKOCYTE COUNT DEVICE

Sensor number	Code
Sensor 1	10101110110001111100110100100000
Sensor 2	00011011110110100011111100100000
Sensor 3	01110010110100001101001100111110

code-multiplexed over a common signal path (Table I). Specifically, each sensor is composed of an array of 5 μm-wide finger electrodes separated by 5 μm gaps, creating local electric fields at the same size scale of leukocytes. The sensors were designed by arranging the sensor electrode sequence based on the corresponding specific 31-bit digital codes: each Coulter sensor is composed of three electrodes, two sensing electrodes, one positive (1's in codes) and one negative (0's in codes) to form a bipolar code signal, and a common electrode meandering in between to excite the whole sensor network (Fig. 3). In this setting, all sensor network data could be simultaneously read from three electrodes. The output waveform was decoded using our custom-built program to identify codes corresponding to individual sensors in the network [23]. After the decoding of sensor data, the cell count for each capture section was determined by subtracting the inlet count from the outlet count.

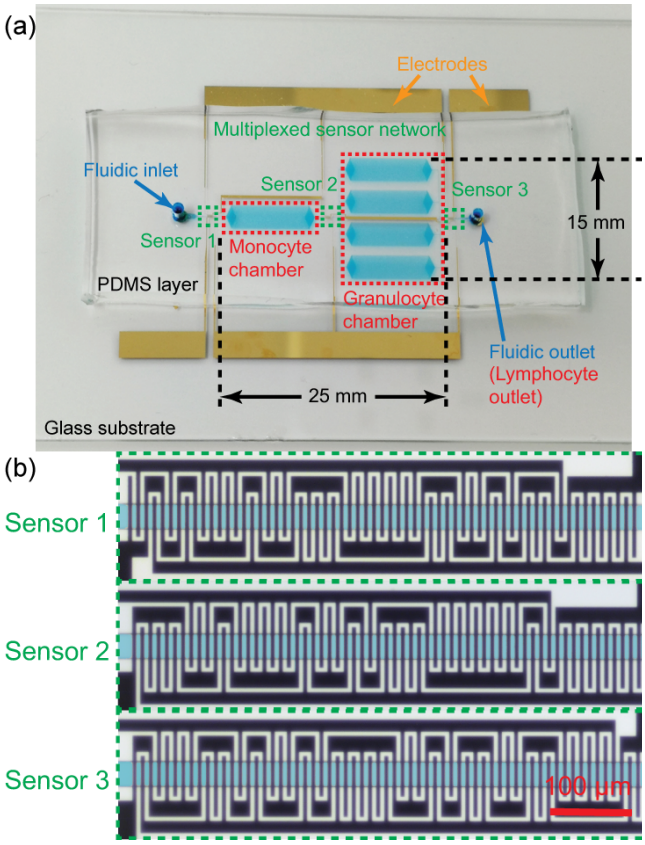

Fig. 3. The photo of the fabricated device filled with blue dye for illustration. (a) The fabricated device is made up of an electrode-patterned glass substrate with a polydimethylsiloxane (PDMS) microfluidic channel layer. Different leukocyte subpopulations will be captured separately in the chambers. (b) Close-up images show the Coulter sensors in the multiplexed sensor network. Each sensor is encoded with a different code as shown in TABLE I (i.e. electrode pattern).

We fabricated the device using a combination of surface micromachining and soft lithography. The device consists of an electrode-patterned glass substrate with a polydimethylsiloxane (PDMS) microfluidic channel layer. The surface electrode on the glass substrate was patterned using a lift-off process. A 1.2 μm-thick NR9 negative photoresist (Futurrex, Inc.) was spun on a 3-inch by 2-inch glass slide, and patterned using a maskless aligner (MLA150, Heidelberg). The glass was then coated with a 20/480 nm Cr/Au stack with e-beam evaporation, and soaked in an acetone batch to remove the sacrificial layer. Separately, the PDMS microfluidic layer was fabricated using soft lithography. A 15-μm thick SU-8 photoresist (SU-8 2015, Microchem) layer was spun on a 4-inch wafer, patterned using a maskless aligner to fabricate the mold. A PDMS prepolymer and crosslinker (Sylgard 184, Dow Corning) were then mixed at a 10:1 ratio, poured onto the mold, degassed, and baked at 65 °C for 4 hours, and peeled off from the mold when cured. The PDMS layer and glass substrate were then activated in oxygen plasma, aligned, and bonded together to form the final device (Fig. 3).

Once the final device is fabricated, the microfluidic chambers were chemically functionalized with the anti-CD33 antibody. Within 10 minutes of the bonding of the PDMS layer and the glass substrate, the chambers were wetted with ethanol (Decon Labs, Inc.) to 1) remove potential air bubbles that might interfere with device operation [24], and 2) enhance the hydrophilicity of the PDMS surface to ensure efficient immobilization of the antibodies [25]. Then, a four-step protocol was used for the crosslinking of the antibodies. First, the channels were treated with (3-aminopropyl)-triethoxysilane (Gelest, Inc.) in ethanol (2% v/v) for 30 minutes. Second, after the chambers were rinsed with ethanol and deionized (DI) water, glutaraldehyde (Sigma-Aldrich) solution in DI water (1% v/v) was introduced into the chamber and incubated for 30 minutes. Third, the device was rinsed with DI water and phosphate buffered silane (PBS), and an anti-CD33 (WM53 clone, Biolegend) solution was introduced and incubated in the device for 1 hour. Fourth, the unbound antibodies were rinsed with PBS, and the chambers were incubated with bovine serum albumin (BSA) to block potential non-specific cell attachment to the device. Finally, the device was rinsed with PBS again to complete the functionalization process.

III. Results And Discussion

A. Calibration of the flow rate for differential leukocyte capture

To determine the sample flow rate for capturing different leukocyte subpopulations in different sections of the device, we calibrated our device using leukocyte suspensions. Blood samples were obtained *via* venipuncture from consenting healthy donors according to the Georgia Tech Institutional Review Board-approved protocol [26]. Following the lysis of red blood cells (RBCs), samples were driven through the device with a syringe pump. A 500 kHz sine wave was applied to excite the sensor network, and current signals from the sensors were measured using a lock-in amplifier. The electric signal was decoded using a custom-built signal processing algorithm to obtain the cell count from each sensor.

In our experiments, we ran the leukocytes at different flow speeds, and monitored the cell capture rate under each tested flow speed (Fig. 4). The total volumetric flow rate in our microfluidic device was controlled by a syringe pump. The flow speed of cells in different capture chambers was then modulated by differences in the effective cross section, which depended on (1) the dimensions of the microfluidic capture and (2) the number of microfluidic channels that were parallel to it. We tested leukocyte capture rates at flow speeds up to 640 μm/s, and found that 1) the leukocyte capture rate decreased with increasing flow speed, 2) the cell capture rate changed dramatically under flow speeds ranging between 5 μm/s to 300 μm/s, and 3) the capture rate tapered to 6% to 9% after 300 μm/s. Specially, for leukocyte flow speed below 30 μm/s, the capture rate ranges between 60% and 70%, which corresponds to the expected fraction of granulocytes and monocytes among leukocytes. Therefore, we concluded that at this flow rate, all leukocytes, except lymphocytes, which lack CD33 antigens, could be differentially captured on the device. Next, we determined the flow speed that can distinguish between granulocytes and monocytes. The expected fraction of monocytes in a leukocyte population is ~10%. Because monocytes have very strong CD33 expression, we expected that only monocytes were capable of attaching to the chip under higher flow rates. From leukocyte capture data, we determined that the fraction of captured leukocytes at flow rates above 120 μm/s was close to the expected fraction of ~10% and was relatively insensitive to changes in the cell flow speed. Based on these experimental findings, we chose 120 μm/s and 30 μm/s as the gating flow rates (corresponding to a volumetric flow rate of 15 μL/h) to distinguish monocytes from other leukocytes and granulocytes from lymphocytes, respectively, and used these parameters for our leukocyte assays.

We also independently validated the identity of immunocaptured cells in different sections of the device *via* fluorescent labeling. Briefly, following the capture of leukocytes on the device, we labeled the captured cells using Alexa Fluor 647 anti-CD33 antibody (WM53 clone, Biolegend) and measured CD33 expression with fluorescence microscopy (Fig. 5). In our analysis, we observed that the leukocytes captured in the first stage of the device (i.e., cells that were treated as monocytes) indeed had significantly higher CD33 expression than the leukocytes that were captured at the second stage under the lower flow rate. These results confirmed the successful spatial separation of leukocytes based on their surface expression in our device.

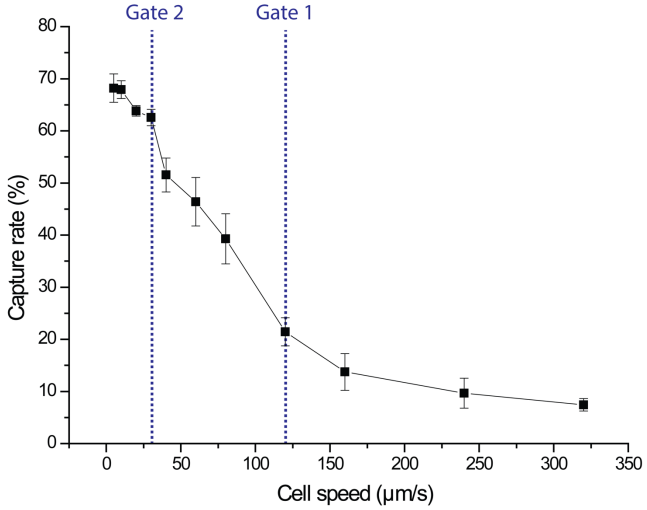

Fig. 4. Capture rate of the cells in the capture chamber at different cell flow speed. The capture rate decreases while we increase the cell speed. The curve can be divided into three segments with different slopes, and the boundaries can be identified from the curve directly. (n=3)

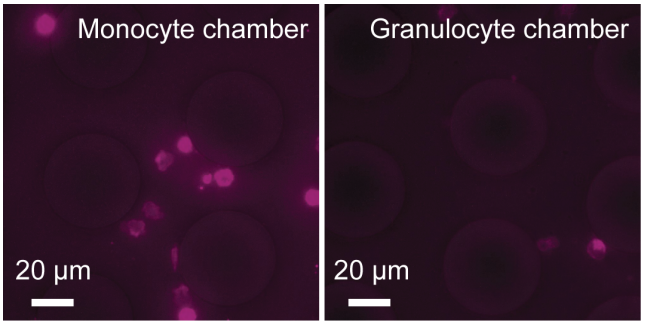

Fig. 5. Fluorescent labeling of the captured cells in the chambers. All the captured cells have been labeled with fluorophore conjugated antibodies, and the cells in the monocyte chambers have higher fluorescent intensity than the cells in the granulocyte chambers. The photos were taken under the same software settings.

B. Different leukocyte count assay

Following the calibration of our device, we applied our technology to determine differential leukocyte count in blood samples collected from another donor. Similar to the previous experimental setup, leukocyte suspension was driven through our microfluidic device using a syringe pump, and we adjusted the flow rate to tune the cell speed in the first and second sections of the device to 120 μm/s and 30 μm/s, respectively.

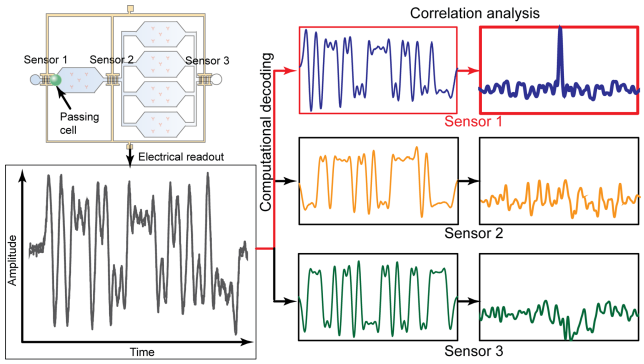

Fig. 6. The decoding process to identify sensor signals from the electrical readout. The cell will generate a waveform dictated to the sensor when it flows over a sensor. The signal readout will be correlated with all the possible waveforms using our algorithm to identify which sensor the cell belongs to. The case in the figure shows the decoding of the signal when a cell flows over Sensor 1.

The electrical data obtained from Microfluidic CODES is used to monitor the spatial information of all the leukocytes in the microfluidic device. As introduced earlier, once a cell comes across a sensor in the network, it will generate a dictated waveform corresponding with that sensor in the electrical signal. By matching the shape of each cell signal waveform with all the possible shapes *via* correlation analysis, we will identify the exact sensor the cell passes (Fig. 6). The data was automatically analyzed using our custom-built decoding program to get the total number of cells passing each sensor, with a total counting accuracy of >97% [27]. Using this method, we first obtained the number of cells detected by each sensor from the electrical data (Table II). By subtracting the number of leukocytes at the exit of a section from the count at the entrance, we calculated the numbers of cells captured in different sections of the device and obtained the number of each leukocyte subpopulation based on our calibration (Table III).

To validate our results, we benchmarked our device against a commercial benchtop hematology analyzer (CELL-DYN, Abbott). We processed matched blood samples using our microfluidic device and performed a complete blood count with the hematology analyzer. We found our results closely matched the results from the hematology analyzer, with a <6% difference for granulocytes and lymphocytes, and a <3% difference for monocytes (Fig. 7).

TABLE II
COUNTS FROM EACH CODED ELECTRICAL SENSOR

Coded sensor number	Cell count
Sensor 1	817
Sensor 2	743
Sensor 3	305

Considering the simplicity of our device, the agreement between results from our method and conventional blood analyzer confirmed the applicability of our technology for differential leukocyte count in point of care settings. It should however be noted that the results could be improved further by fine tuning the ratio between the two flow rates between different sections of our device. For example, our overestimation of monocytes and underestimation of granulocytes can simultaneously be improved by increasing the flow rate ratio between the first and second sections of the device in the device design stage. From our results, a flow speed ratio of ~5.4:1 (135 μm/s and 25 μm/s in the first and second sections, respectively) would produce a result with a closer fit with the one from the commercial system. Finally, the flow rates and chamber dimensions in this work are optimized for CD33-based fractionation of leukocytes into monocytes, granulocytes, and lymphocytes, and therefore different target cells or antigens could be achieved following a similar calibration process.

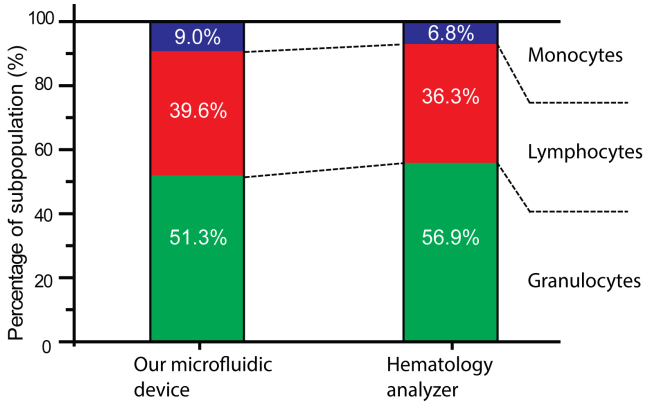

Fig. 7. The frequency of leukocyte subpopulations measured by our device and a commercial hematology analyzer on the matched blood sample.

IV. CONCLUSION

In this paper, we introduced an electrically readable microfluidic assay for the differential leukocyte counts with no pre-labeling. In our device, we utilized varying CD33 expression of leukocyte subgroups to fractionate the sample *via* immunocapture. To ensure differential immunocapture of leukocytes based on their surface antigen expressions, our device was designed to modulate cell flow speeds at different locations on the chip. By counting the number of captured leukocytes at different locations on the chip through an

TABLE III
DIFFERENTIAL LEUKOCYTE COUNTS OBTAINED USING OUR DEVICE

Chamber	Cell count	Percentage	Cell type
Monocyte chamber	74	9.0%	Monocytes
Granulocyte chamber	438	51.3%	Granulocytes
Lymphocyte outlet	305	39.6%	Lymphocytes

integrated electrical sensor network, the results could be obtained from an electrical waveform. Benchmarking our technique against commercial systems validated the accuracy of our approach. Unlike current methods, our assay uses a glass slide-sized chip and significantly simplifies obtaining differential leukocyte counts.

While this paper focused on CD33-based differentiation of leukocyte subpopulations, our work provides a platform technology that can be adapted to analyze any heterogeneous cell mixture. By modifying the device geometry, sample flow speed, and surface chemistry (i.e., multiple antibodies), our device can be used for further differentiation of leukocyte subsets or analysis of populations other than blood cells. Furthermore, by integrating sample preparation steps such as RBC lysis [28] into the chip, it is possible to create sample-to-answer assays. Taken together, compared to the conventional flow cytometry and manual cytometry methods, our device does not need any cell pre-labeling and provides an integrated assay for simple and accurate cytometry in resource-limited and point-of-care settings.

ACKNOWLEDGMENT

The authors would like to thank Georgia Tech Stamp Health Services for the support of this work.

REFERENCES

[1] P. Dutta, and M. Nahrendorf, "Regulation and consequences of monocytosis," *Immunol. Rev.*, vol. 262, no. 33, pp. 167-178, Nov. 2014.

[2] J. Bux, K. Kissel, K. Nowak, U. Spengel, and C. Mueller-Eckhardt, "Autoimmune neutropenia: clinical and laboratory studies in 143 patients," *Ann. Hematol.*, vol. 63, no. 5, pp. 249-252, Nov. 1991.

[3] R. T. Lewis, and H. Klein, "Risk factors in postoperative sepsis: Significance of preoperative lymphocytopenia," *J. Surg. Res.*, vol. 26, no. 4, pp. 365-371, Apr. 1979.

[4] M. Toner, and D. Irimia, "Blood-on-a-chip," *Annu. Rev. Biomed. Eng.*, vol. 7, pp. 77-103, Aug. 2005.

[5] D. Huh, W. Gu, Y. Kamotani, J. B. Grotberg, and S. Takayama, "Microfluidics for flow cytometric analysis of cells and particles," *Physiol. Meas.*, vol. 26, no. 3, pp. R73-R98, Feb. 2005.

[6] W. Shi, L. Guo, H. Kasdan, and Y. C. Tai, "Four-part leukocyte differential count based on sheathless microflow cytometer and fluorescent dye assay," *Lab Chip*, vol. 13, no. 7, pp. 1257-1265, Apr. 2013.

[7] M. L. Balter, A. I. Chen, A. Colinco, A. Gorshkov, B. Bixon, V. Martin, A. Fromholtz, T. J. Maguire, and M. L. Yarmush, "Differential leukocyte counting via fluorescent detection and image processing on a centrifugal microfluidic platform," *Anal. Methods*, vol. 8, no. 47, pp. 8272-8279, Dec. 2016.

[8] X. Liu, X. Huang, Y. Jiang, H. Xu, J. Guo, H. W. Hou, M. Yan, and H. Yu, "A microfluidic cytometer for complete blood count with a 3.2-megapixel, 1.1-µm-pitch super-resolution image sensor in 65-nm BSI CMOS," *IEEE Trans. Biomed. Circuits Syst.*, vol. 11, no. 4, pp. 794-803, Apr. 2017.

[9] W. H. Coulter, "High speed automatic blood cell counter and cell size analyzer," *Proc. Natl. Electron. Conf.*, vol. 12, 1034, Oct. 1956.

[10] D. Holmes, D. Pettigrew, C. H. Reccius, J. D. Gwyer, C. van Berkel, J. Holloway, D. E. Davies, and H. Morgan, "Leukocyte analysis and differentiation using high speed microfluidic single cell impedance cytometry," *Lab Chip*, vol. 9, no. 20, pp. 2881-2889, Oct. 2009.

[11] U. Hassan, B. Reddy, Jr., G. Gamhorst, O. Sonoiki, T. Ghonge, C. Yang, and R. Bashir, "A microfluidic biochip for complete blood cell counts at the point-of-care," *Technology*, vol. 3, no. 4, pp. 201-213, Dec. 2015.

[12] X. Han, C. van Berkel, J. Gwyer, L. Capretto, and H. Morgan, "Microfluidic lysis of human blood for leukocyte analysis using single cell impedance cytometry," *Anal. Chem.*, vol. 84, no. 2, pp. 1070-1075, Jan. 2012.

[13] BD Sciences, "Human and Mouse CD Marker Handbook." [Online]. Available: https://www.bdbiosciences.com/documents/cd_marker_handbook.pdf, Accessed on: July 2020.

[14] C. Cozens-Roberts, D. A. Lauffenburger, J. A. Quinn, "Receptor-mediated cell attachment and detachment kinetics. I. Probabilistic model and analysis," *Biophys. J.*, vol. 58, no. 4, pp. 841-856, Oct. 1990.

[15] Y. Zhang, V. Lyons, D. Pappas, "Fundamentals of affinity cell separations," *Electrophoresis*, vol. 39, no. 5-6, pp. 732-741, Mar. 2018.

[16] R. Liu, N. Wang, F. Kamili, and A. F. Sarioglu, "Microfluidic CODES: a scalable multiplexed electronic sensor for orthogonal detection of particles in microfluidic channels," *Lab Chip*, vol. 16, no. 8, pp. 1350-1357, Apr. 2016.

[17] N. Wang, R. Liu, and A. F. Sarioglu, "Microfluidic platform with multiplexed electronic detection for spatial tracking of particles," *J. Vis. Exp.*, vol. 121, e55311, Mar. 2017.

[18] O. Civelekoglu, N. Wang, M. Boya, T. Ozkaya-Ahmadov, R. Liu, and A. F. Sarioglu, "Electronic profiling of membrane antigen expression via immunomagnetic cell manipulation," *Lab Chip*, vol. 19, no. 14, pp. 2444-2455, Jul. 2019.

[19] R. Liu, C. H. Chu, N. Wang, T. Ozkaya-Ahmadov, O. Civelekoglu, D. Lee, AKM Arifuzzman, and A. F. Sarioglu, "Combinatorial immunophenotyping of cell populations with an electronic antibody microarray," *Small*, vol. 15, no. 51, 1904732, Dec. 2019.

[20] R. Gold, "Optimal binary sequences for spread spectrum multiplexing," *IEEE Trans. Inf. Theory*, vol. 13, no. 4, pp. 619-621, Oct. 1967.

[21] R. Gold, "Maximal recursive sequences with 3-valued recursive cross-correlation functions," *IEEE Trans. Inf. Theory*, vol. 14, no. 1, pp. 154-156, Jan. 1968.

[22] R. Liu, W. Waheed, N. Wang, O. Civelekoglu, M. Boya, C. H. Chu, and A. F. Sarioglu, "Design and modeling of electrode networks for code-division multiplexed resistive pulse sensing in microfluidic devices," *Lab Chip*, vol. 17, no. 15, pp. 2650-2666, Jul. 2017.

[23] R. Liu, N. Wang, N. Asmare, and A. F. Sarioglu, "Scaling code-multiplexed electrode networks for distributed Coulter detection in microfluidics," *Biosens. Bioelectron.*, vol. 120, pp. 30-39, Nov. 2018.

[24] R. Liu, "Electronic antibody microarrays for label-free cell immunophenotyping," Ph.D. dissertation, Bioeng., Georgia Tech, the Institute, Atlanta, GA, USA, 2020.

[25] J. Zhou, A. V. Ellis, N. H. Voelcker, "Recent developments in PDMS surface modification for microfluidic devices," *Electrophoresis*, vol. 31, pp. 2-16, Jan. 2010.

[26] The Georgia Institute of Technology, Institutional Review Boards. [Online], Available: https://researchintegrity.gatech.edu/irb, Accessed on July 2020.

[27] N. Wang, R. Liu, N. Asmare, C. H. Chu, A. F. Sarioglu, "Processing code-multiplexed Coulter signals via deep convolutional neural networks," *Lab Chip*, vol. 19, pp. 3292-3304, Aug. 2019.

[28] L. Nan, Z. Jiang, X. Wei, "Emerging microfluidic devices for cell lysis: a review," *Lab Chip*, vol. 14, pp. 1060-1073, Mar. 2014.

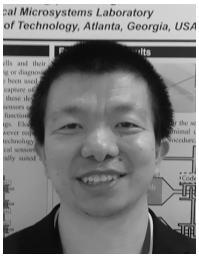

Ruxiu Liu received the B.S. degree from Northeastern University, Shenyang, China, in 2011, and the M. S. degree from Zhejiang University, Hangzhou, China, in 2014, both in control engineering. He is currently pursuing the Ph.D. degree in bioengineering and biomedical engineering at the Georgia Institute of Technology, Atlanta, GA, from 2014. His current research interest includes lab-on-a-chip and point-of-care medical devices, biosensors and bioelectronics, and the interaction between culture and medical techniques.

A K M Arifuzzman received the B.S. degree from American International University-Bangladesh (AIUB), Bangladesh, in 2011, and the M.S. degree from the University of Alabama at Birmingham, USA, in 2016, both in electrical Engineering. He is currently working towards Ph.D. degree at the Georgia Institute of Technology with the Biomedical Microsystems Laboratory. His research interests include BioMEMS, Bioelectronics, and Microfluidics.

Ningquan Wang received his B.S. degree in Electrical Engineering and Automation from Nanjing University of Science & Technology in 2012. He received his M.S.E.E degree from Brown University in 2014. He is currently a Ph.D. student in the School of Electrical and Computer Engineering at the Georgia Institute of Technology. He has a great interest in designing bio-medical microdevices that utilize signal processing and computation to address healthcare needs.

Ozgun Civelekoglu received the B.S. degree in Electrical and Electronics Engineering from Koc University, Turkey in 2016, and the M.S. degree in Electrical and Computer Engineering from Georgia Institute of Technology, Atlanta, GA, USA in 2018. He is currently pursuing the Ph.D. degree with Biomedical Microsystems Laboratory at the Georgia Institute of Technology, under the supervision of Dr. A. Fatih Sarioglu. His current research includes microflow cytometry and cell sorting for point-of-care testing.

A. Fatih Sarioglu (M'10) received the B.Sc. degree from Bilkent University, Ankara, Turkey, in 2003, and the M.S. and Ph.D. degrees from Stanford University, in 2005 and 2010, respectively, all in electrical engineering. He was a Postdoctoral Research Associate with the Center for Nanoscale Science and Engineering, Stanford University, from 2010 to 2012. From 2012 to 2014, he was a Research Fellow with the Center for Engineering in Medicine, Massachusetts General Hospital, and Harvard Medical School. In October 2014, he joined the School of Electrical and Computer Engineering, Georgia Institute of Technology, as an Assistant Professor. His research interest includes the interface of nano-/microengineering and biomedicine. He is particularly interested in developing N/MEMS-based technologies for biomedical applications.